Optical studies of the growth of $Cd_{1-x}Zn_xS$ nanocrystals in borosilicate glass

Hikmet Yükselici, P. D. Persans, and T. M. Hayes
Department of Physics, Rensselaer Polytechnic Institute, Troy, New York 12180-3590
(Received 23 May 1995)

We analyze optical-absorption and Raman-scattering measurements of CdS- and Zn-doped borosilicate glass, heat treated at 600 °C to 725 °C, to study the nucleation and growth of II-VI nanoparticles. The energy of vibrational Raman modes indicates that $Cd_{1-x}Zn_xS$ crystallites form where x is initially zero and increases to 0.15 with time. In glass which is quenched from high temperature (> 1000 °C) there is a weak, monotonic optical absorption which increases with photon energy. Heat treatment at 600 °C to 725 °C causes the optical absorption to increase and to form a peak between 3.0 and 3.2 eV. After the peak reaches its maximum value, it begins to shift to lower energy. We interpret the optical data in terms of quantum confinement of electron and hole excited states. We conclude that nucleation of particles in this glass composition is homogeneous. Typical critical nuclei are in the range from 1.5 to 2 nm. The particle size distribution is narrowest (25% full width at half maximum) at the end of the homogeneous nucleation stage and broadens when coarsening begins.

INTRODUCTION

When semiconductor particles are reduced in scale to nanometer dimensions, their linear and nonlinear optical and electro-optical properties differ markedly from those of bulk crystals of the same composition. The thrust of fundamental studies of such systems has been to develop an understanding of the basic electronic, optical, and vibrational properties and to develop theoretical approaches and approximations which will allow us to predict the properties of new and potentially useful systems. The basic technological goal is to control optoelectronic and vibrational properties so that materials can be tailored for optical, electro-optical, and nonlinear optical applications in communications, computing, and traditional optics. The principal current application of nanoparticle semiconductor-doped glasses is as long-wavelength-pass optical filters.[1] An important potential application is as nonlinear optical elements in communications or computing systems.[2–10] Nanocrystalline composites have been shown to exhibit significant third-order optical nonlinearities and picosecond free-carrier lifetime.[6,11–21]

For applications, it is necessary to gain understanding of and control over the properties of large collections of nanocrystals. For example, the resonant nonlinear optical response of a composite will be dispersed and decreased if all crystallites in a device do not have the same resonance energy. Size distribution of crystallites is the primary source of inhomogeneous broadening in both powders[22] and doped-glass composites.[23–26] One of the major goals of materials development of nanocrystallite systems must therefore be to decrease the width of the size distribution for small particles. One approach to synthesis which has yielded potentially useful quantum dots is the precipitation of II-VI and I-VII semiconductors from a solid or liquid solution. Although the Cd(S,Se) family of nanocrystals has been extensively investigated, there remain many open questions and technical opportunities.

The limits on particle size and size distribution depend on the processes by which particles are formed and grow. For example, homogeneous nucleation yields an initial size distribution which is Gaussian with a width which depends only on surface tension. Crystallite nucleation in glasses is usually inhomogeneous, but it is not yet clear whether such behavior dominates the properties of II-VI-doped glasses or how it can be modified.

In this paper we report a study of the nucleation and growth of II-VI-doped borosilicate glass. Our principle tools are optical absorption and Raman scattering. Our goals are both to elucidate the type of information one can gather from optical studies and to identify general growth patterns, such as nucleation mode, which can be used to classify and control materials properties.

NUCLEATION AND GROWTH PROCESSES

Several approaches to the synthesis of II-VI nanoparticles have been explored, including precipitation from liquid solution,[27] solid-phase precipitation,[28] and growth in a confining zeolite structure.[9] Very narrow size distributions of CdSe particles with average diameters from 1 to 10 nm have recently been prepared by liquid phase nucleation and selective precipitation with frequent sampling and corrections to the growth conditions during growth.[29]

Solid phase precipitation of CdS_xSe_{1-x} in borosilicate glass is one of the best known and widely used preparation routes.[1,24,26,28,30–37] It has been used for many years to prepare commercially available colored glass edge filters (for example, products from Schott Glass Technologies, Corning, Hoya). These systems differ from "wet" preparations in a few key points. First, the typical nucleation and growth temperatures are in the 500–800 °C range whereas wet preparations are generally confined to temperatures below 200 °C. This difference in temperature may lead to different classes of dominant defects and/or crystal structures. Second, it is relatively

straightforward to grow particles in glass which are solid solutions of CdS, CdSe, and CdTe,[1,36,37] whereas the growth of ternary or quaternary semiconductor nanocrystals by wet techniques has not yet been widely investigated. Third, the interface of the crystallite with the solid (glass or crystal) host will have different steric and chemical properties compared to bare or capped crystallites.

There are essentially four stages which are identified in the literature on the preparation of nanocrystalline CdS/glass samples.[23,32–35,38]

First, Cd and S are dissolved into the glass at high temperature ($T > 1100\,^{\circ}\mathrm{C}$ for borosilicate glass) and a supersaturated metastable solution of unknown species is formed by quenching to room temperature. For glasses, the maximum available concentration of Cd and S depends on the solubility of these elements of their compounds at the founding temperature. The temperature at which the reactants are in equilibrium with large bulklike crystallites in the melt is called the equilibrium temperature T_0.

Second, nuclei are formed by heat treatment. It has recently been proposed[39,40] that the origin of the nuclei is fluctuation in the local concentrations of reactants, but the conventional point of view is that nuclei are extrinsic.[32,38]

Third, if nuclei are extrinsic, then the number depends on initial conditions and we would expect the particles to grow by diffusion of reactants to the surface. In this stage, the number of particles does not change, while the average radius of the particles increases according to $R^2 = K_1 t + R_0^2$, where R_0 is the initial radius and K_1 is the normal growth coefficient.[45] If one neglects R_0, then the average particle size grows as[40]

$$R(t) = \left[2D \frac{C_0 - C_e}{C_p - C_e} t \right]^{1/2} , \tag{1}$$

where C_0 is the concentration of the limiting reactant in the matrix at $t = 0$, C_e is the equilibrium concentration of limiting reactant in the glass matrix, C_p is the concentration of limiting reactant in the particle, and D is the diffusion coefficient for the limiting reactant. The concentration of reactants decreases during this stage.

If nuclei are formed by thermodynamic concentration fluctuations (homogeneous nucleation), only those nuclei will grow whose radius exceeds a critical value:[41]

$$R_c = - \left[\frac{2\sigma}{\Delta G_v} \right] , \tag{2a}$$

where ΔG_v is the bulk free energy decrease per unit volume and σ is the interface energy per unit area. If we assume that the entropy of fusion is independent of temperature, then the critical radius at constant pressure can be expressed as[42]

$$R_c(T) = \frac{2\sigma V_m}{\Delta H} \left[\frac{T_0}{T_0 - T} \right] , \tag{2b}$$

where V_m is the mean specific volume of material in a particle, and ΔH is the heat of fusion. During this stage, the average size of the particle distribution does not change with time but the number of particles increases with time.[43,44] The rate at which particles of the critical radius form is given by

$$I = K e^{-(\Delta G_c + \Delta G_a)/kT} ,$$

where

$$K = n_c n \nu_0 (a\sigma / 9\pi kT) \tag{3}$$

and

$$\Delta G_c = 16\pi\sigma^3 / 3(\Delta G_v)^2 .$$

ΔG_c is the free energy necessary to form a critical nucleus, ΔG_a is the free energy of activation to cross the interface, n_c is the number of molecules in the surface of the nucleus, n is the number of molecules per unit volume in the glass, a is a geometrical factor, and ν_0 is the attempt frequency for an atom to cross from the glass to the crystal.[41]

Homogeneous nucleation theory[43,45] predicts that the standard deviation of the Gaussian particle size distribution during this nucleation stage should be given by

$$\Delta R = (3kT / 8\pi\sigma)^{1/2} \tag{4}$$

and the full width at half maximum is given by $\Delta R_{1/2} = (2 \ln 2)^{1/2} \Delta R$. Note that the width of the size distribution depends only on the ratio of interface tension to thermal energy and decreases with increasing interface energy.

Finally, after available Cd and/or S concentration has dropped below a given level, larger particles continue to grow while smaller particles dissolve. This final stage is known as the coarsening or ripening stage. During this stage, the average radius R is equal to the critical radius which increases according to[43,46]

$$R(t) = \left[\frac{4\alpha D}{9} \right] t^{1/3} , \tag{5}$$

where $\alpha = 2\sigma v^2 C_e / kT$ and the total number of particles drops off as $1/t$. The particle size distribution during this coarsening phase is described by the Lifshitz-Slyozov formula:[23,43,46]

$$P(u) = 3^4 2^{-5/3} e u^2 (u+3)^{-7/3} \left(\tfrac{3}{2} - u\right)^{-11/3} \times \exp\left((2u/3 - 1)^{-1}\right) \quad \text{for } u < \tfrac{3}{2} \tag{6a}$$

and

$$P(u) = 0 \quad \text{for } u > \tfrac{3}{2} \tag{6b}$$

where $u = r / R_c$, r is the particle radius, and R_c is the critical radius. Note that this function produces an asymmetric distribution in r with peak at $\approx 1.2 R_c$ and full width at half maximum of $\approx 0.5 R_c$.[43]

REVIEW OF PREVIOUS EXPERIMENTAL STUDIES

The earliest studies of particle formation in Cd(S,Se)-doped glasses focused on the conditions which lead to nu-

cleation and growth[33,34] but did not report extensive information on the optical properties of the resultant glasses. These early studies focused on Cd(S,Se) particles formed in glasses which contained significant amounts of Zn; most commercial glasses contain Zn as well as Cd and S. The standard model developed from these studies proposes that heterogeneous nucleation is followed by diffusion-limited growth.

Borelli *et al.*[1] reported the preparation of CdS and CdSe nanocrystals in Zn-containing glass and demonstrated correlation between particle size and optical band gap (quantum confinement). They reported the size distribution in one commercial (CS 2-61) sample and found a standard deviation in radius of 1.25 nm for an average radius of 5 nm. TEM measurements on experimental heat-treated CdSe-doped glasses produced 2.2-nm average radius with 0.6-nm standard deviation and 4-nm radius with 1.1-nm standard deviation, respectively. Borelli *et al.* also observed that the optical band edge for their CdS-doped glass started well above the bulk band gap for CdS and moved first toward the bulk band gap and, after long anneals at high temperature, began to move to higher energy again. They observed that the lattice constant decreased during this last stage and proposed that Zn incorporation was responsible for both band-edge shift and lattice contraction.

More recent studies have attempted to correlate different growth regimes with optical properties. Ekimov[28] and Potter and Simmons[24] studied the evolution of size and optical properties of CdS in zinc-free borosilicate glass during the coarsening stage of growth, well after nucleation was complete. They found that the size evolution and size distribution were consistent with Lifshitz-Slyozov ripening.

Sukumar and Doremus[47] studied the evolution of the optical edge of CdS-doped borosilicate glass which contained a large amount (10%) of Zn but did not report on Zn content of the particles. They observed very large blueshifts of the optical edge which they interpreted as quantum size shift in very small particles. Sukumar and Doremus found that the absorption edge shifted linearly in $1/t$, suggesting diffusion-limited growth on extrinsic nuclei. The activation energy for growth was estimated to be 273 kJ/mol (2.8 eV).

Gurevich *et al.*[40] studied x-ray diffraction and the optical-absorption edge in CdS in SiO_2 and CdS in borosilicate glass. They concluded that early stages of particle formation were controlled by homogeneous nucleation, giving way to diffusion-limited growth at later times. The equilibrium temperature was found by applying homogeneous nucleation theory [Eq. 2(b)]. Their CdS-doped borosilicate glass had equilibrium temperature of 900 °C, whereas the equilibrium temperature of SiO_2 films ranged from 1650 °C to 2000 °C with critical radii of 2–3 nm at 1000 °C. Gurevich *et al.* did not analyze the size distribution or report enough optical data to permit independent analysis.

Fuyu and Parker[35] studied CdS_xSe_{1-x} particle growth in Zn-doped glass and found that the optical-absorption edge shifted in a manner consistent with diffusion-limited growth at early stages and coarsening at later stages. They found an activation energy for growth of 250 kJ/mol, which they associated with the diffusion coefficient for the limiting reactant. Detailed analysis of this system is expected to be problematic because the S to Se ratio of the crystallites may not be constant and Zn may be incorporated into crystallites. Fuyu and Parker did not report on these effects.

Liu and Risbud[45] analyzed TEM measurements on CdSe particles in borosilicate glass and found that the early size distribution for a single sample was consistent with homogeneous nucleation theory. For heat-treatment temperature of 760 °C, they found an average particle radius of 2.5 nm and distribution width (FWHM) of 1.4 nm. They were able to fit their measurements with homogeneous nucleation parameters $\sigma = 8.7 \times 10^{-4}$ J/m^2 and $\Delta G_v = 7 \times 10^5$ J/m^3.

There have been a few reports on the average size and size distribution of CdS_xSe_{1-x} nanoparticles,[23,26] but there is insufficient information on thermal history in these reports for us to extract growth model parameters.

EXPERIMENTAL DETAILS

All of the samples for this study were cut from a single homogeneous, unstruck CdS-doped glass sample (4 cm thick) which was supplied by Schott Inc. The Si, Na, Ca, K, Zn, and O content of the glass was determined by electron microprobe.[48] The boron concentration was estimated indirectly by assuming that O is incorporated in the stoichiometric oxides: SiO_2, B_2O_3, Na_2O, CaO, K_2O. Oxygen, which could not be assigned to Si, Na, K, and Ca, was assigned to B yielding molecular concentrations of 60% SiO_2, 20% B_2O_3, 8% Na_2O, 6% CaO, 4% K_2O, 0.4% ZnO. The Cd content was 1.1×10^{19} cm^{-3}, measured by x-ray absorption both before and after heat treatments.[49,50]

Small samples (0.5 to 2 mm thick) were cut from this large sample and heat treated in air at various temperatures from 600 °C to 725 °C. A platinum foil was used to isolate samples from the ceramic boat during heat treatment. The samples were polished on both sides after heat treatment.

Optical-absorption coefficients were deduced from optical transmission measurements which were carried out at room temperature on a Perkin Elmer 330 UV spectrophotometer. Raw optical density data were reduced by subtracting the baseline due to reflection and correcting for the thickness of the sample to find the absorption coefficient. For derivative spectra, the absorption data were first smoothed using a seven-point algorithm.

Resonant Raman-scattering measurements were carried out at room temperature using a 2000M Jobin-Yvon ISA double monochromator with photon-counting detection electronics. The excitation sources included a HeCd (442 nm) laser, and an Ar ion laser (458, 476, 488, 514.5 nm). Most measurements were carried out with the HeCd laser. Details of resonant Raman measurements can be found elsewhere.[51–53]

EXPERIMENTAL RESULTS

In Fig. 1, we show the results of absorption measurements between 2.5 and 3.5 eV for a series of samples heat treated at several temperatures from 600 °C to 725 °C for various times from 15 min to many days.

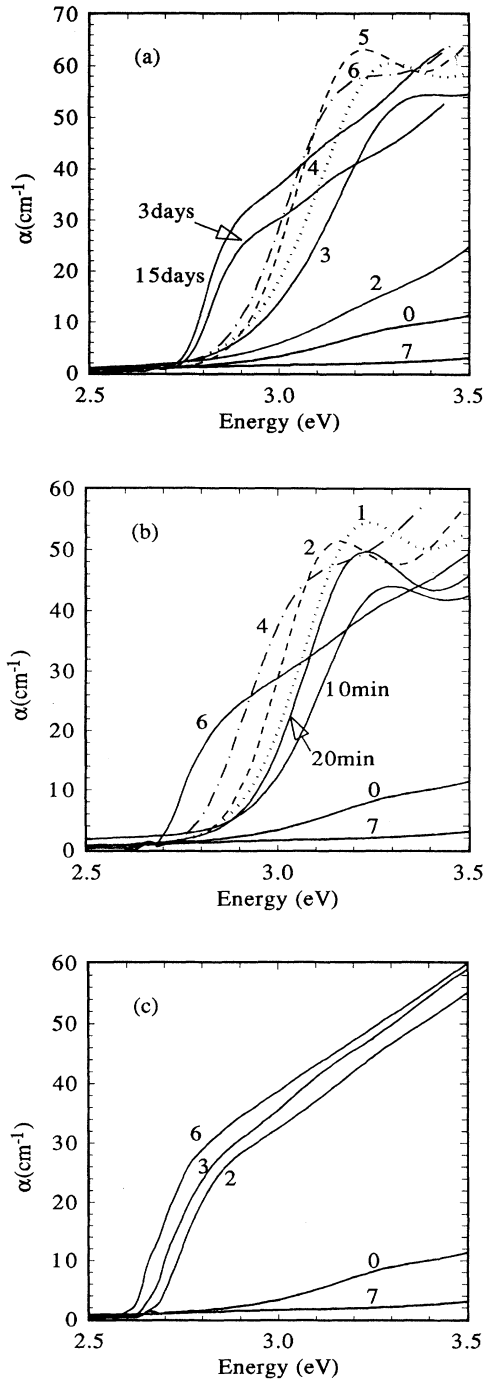

FIG. 1. Absorption spectra for CdS/glass samples heat treated at (a) 600 °C, (b) 650 °C, and (c) 700 °C. Key: 0→ as received, 1→15 min, 2→30 min, 3→1 hr, 4→2 H, 5→4 h, 6→ overnight (12–15 h), 7→ melted at 1100 °C for 9 min and quenched to room temperature.

For no heat treatment by us (unstruck glass) the absorption rises slowly and monotonically with increasing photon energy starting with a value close to zero (<1 cm^{-1}) at 2.8 eV to a value of 12 cm^{-1} at 3.5 eV. When the glass is heat treated at 1100 °C and quenched rapidly to room temperature, the absorption decreases at all energies. Absorption characteristic of particles can be restored by heat treatment at 600–700 °C.

With increasing heat treatment time at temperatures between 600 °C and 675 °C, the absorption coefficient increases until a peak between 3 and 3.5 eV is observed. With longer annealing, the magnitude of the peak decreases and the absorption edge moves to lower energies. After very long times, the rate at which the absorption edge shifts slows dramatically. The asymptotic position of the absorption edge is 2.6–2.7 eV, depending on heat treatment temperature. This asymptote energy decreases with increasing heat treatment temperature.

The peak or shoulder in the absorption spectra was identified by taking the first minimum in the second derivative of each spectrum. In Fig. 2 we show the second derivative plots of three samples. In Fig. 3, we show the energy of the peak or shoulder, determined by the position of the first minimum in the second derivative, plotted as a function of the logarithm of the heat treatment time for several temperatures.

In Fig. 4 we plot the magnitude of the lowest energy peak of the absorption spectra, for samples heat treated at 600, 625, 650, and 675 °C, respectively, versus the logarithm of the heat treatment time in minutes. From Fig. 4 we observe that the magnitude of the absorption peak reaches a maximum of 47, 54, 59, and 62 cm^{-1} after 10, 20, 90, and 250 min, respectively, for 675, 650, 625, and 600 °C series. The magnitude of the maximum value increases monotonically for decreasing heat treatment temperature. The time at which the maximum is achieved

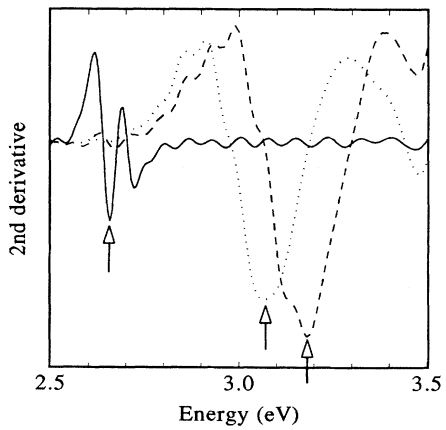

FIG. 2. Second derivative of absorption spectra for three CdS/glass samples heat treated as follows: — — —, 600 °C for 4h; · · · ·, 675 °C for 10 min; ——, 725 °C for 15.5 h. The position of the peak or shoulder is marked on each curve.

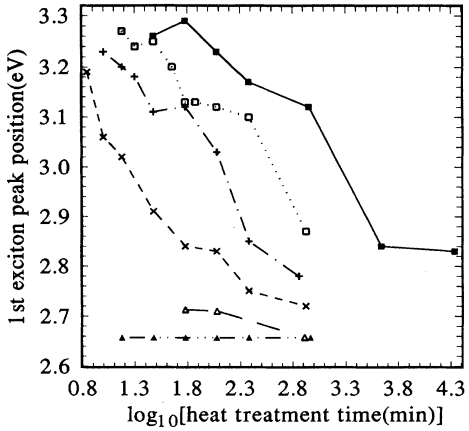

FIG. 3. Shoulder or peak positions of absorption spectra, determined by the position of the first minimum of the second derivative spectra, plotted against heat treatment time. ■, 600 °C; □, 625 °C; +, 650 °C; ×, 675 °C; △, 700 °C; ▲, 725 °C.

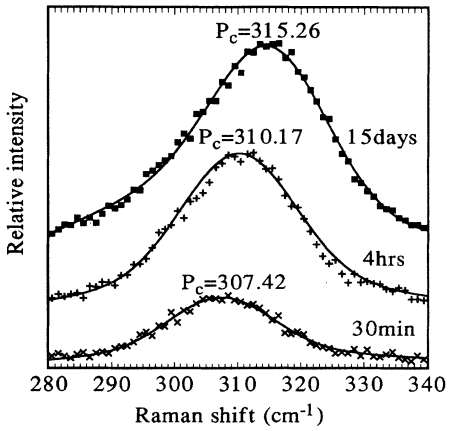

FIG. 5. Typical Raman spectra. ■, 600 °C; +, 650 °C; ×, 675 °C. Solid lines are Gaussian fits to the data points. (P_c is the position of peak center in wave numbers.)

increases dramatically with decreasing temperature. We have excluded the 700 °C and 725 °C data from Fig. 4 because there is no clear peak in the spectra of these series.

Raman-scattering measurements give direct information on the local composition of the crystallites. In Fig. 5 we show Raman spectra for three samples. All three of these spectra were excited with the 2.8 eV (442 nm) line of the HeCd laser. Data points are shown and the solid lines through the data are the result of a fit to a broad quadratic background function and a single narrow Gaussian peak. The narrow peak near 300 cm^{-1} shift is due to the zone-center longitudinal optic mode of CdS. The Raman intensity is resonant for excitation near the optical-absorption edge. We observe in Fig. 5 that the peak position shifts to greater values with longer heat treatment and/or higher temperature. There are three possibilities for this shift: (i) Zn incorporation into the nanocrystals,[54] (ii) compressive strain,[55–57] and (iii) phonon confinement.[58,59] Because the zone-center optical phonon is at a maximum in the phonon-dispersion curve, we expect phonon confinement to lead to a decrease in phonon energy below the bulk value of 303 cm^{-1} as size is reduced. This cannot explain the shift above 303 cm^{-1}. Zn incorporation and compressive strain can both lead to positive shift in the Raman peak position. We propose that the effect observed here is due to Zn incorporation because analysis of EXAFS results on this system[49,50] indicates that there is no change in the nearest-neighbor distance with heat treatment time as would be expected for compression.

In Fig. 6 we show the Raman peak value plotted against the logarithm of the heat treatment time at 625 and 675 °C. The shift is greater for longer time and higher temperature. For Raman shifts between 303 and 320 cm^{-1} the Raman shift in bulk $Cd_{1-x}Zn_xS$ crystals is nearly linear in x,[60] obeying the equation $x=0.013(R_S-303)$ where R_S (cm^{-1}) is the Raman shift. We propose that the increasing Zn content is related to the depletion of Cd in the glass which shifts the thermodynamic equilibrium so that more Zn can be incorporat-

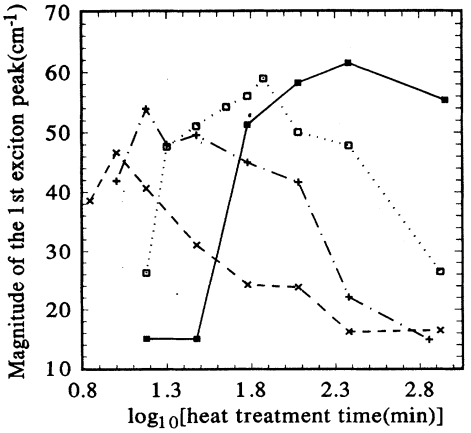

FIG. 4. Peak magnitude of absorption spectra plotted against heat treatment time. ■, 600 °C; □, 625 °C; +, 650 °C; ×, 675 °C.

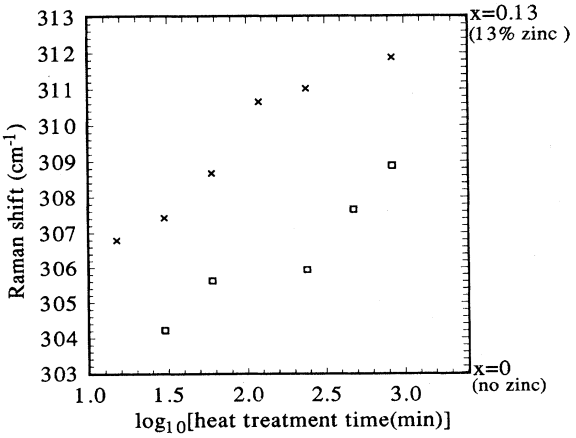

FIG. 6. Raman peak shift plotted against logarithmic heat treatment time. □, 625 °C; ×, 675 °C.

ed into crystallites. This proposal is supported by the fact that excitation with different laser energies, which are resonant with different portions of the particle size distribution, yields the same phonon shift for a given sample. We note that such shifts might also arise from high density of defects such as interstitials or vacancies. Crystallites grown from Zn-free glass show no such shift.

Zn incorporation influences the interpretation of optical properties. The most important change is in the value of the bulk band gap.[54] The largest Raman shift which we observed of 315 cm^{-1} corresponds to Zn content $x=0.15$. In this region, the band gap of $Cd_{1-x}Zn_xS$ depends nearly linearly on x, obeying the relation $E_g=2.45+1.6x$. For $x=0.12$, we expect $E_g=2.65$ eV, consistent with our observations on the optical-absorption edge after long treatments and/or higher temperature (Fig. 1).

MODELING OF THE ABSORPTION SPECTRA

Optical-absorption spectra were simulated using a simple model in order to permit us to deduce particle size and particle size distribution from the shape of the optical-absorption edge. We assume that the optical absorption of the composite is a superposition of the effective medium absorption for a distribution of small spherical noninteracting particles in a nonabsorbing dielectric. We further assume that the real part of the dielectric constant of the particles is size independent. We also assume that the oscillator strength per state is independent of the size of the particle.[61]

In order to link optical data to particle size, we compute the energies of the five lowest energy excited states using the following expression:[5]

$$E_{(n_e,l_e),(n_h,l_h)}=E_b+\frac{\hbar^2}{2R^2}\left[\frac{x^2_{n_e,l_e}}{m_e}+\frac{x^2_{n_h,l_h}}{m_h}\right], \quad (7)$$

where the x's are the roots to the spherical Bessel function. E_b is the bulk band gap (2.45 eV for CdS). Transitions which we include are $(1s,1s)$, $(1p,1p)$, $(1d,1d)$, $(1f,1f)$, and $(2s,2s)$ for both normal and spin-orbit split valence bands. Values of $0.2m_0$ and m_0 are used for m_e and m_h, respectively. We use the bulk CdS value of 60 meV for the spin-orbit splitting. These values are consistent with experimental data on particle sizes between 1 and 3 nm in radius.[9,32] To compute the absorption for one particle, we assume that each transition gives rise to a homogeneously broadened Gaussian absorption band and we add the absorption bands together. Although five excited states with spin-orbit coupling are included in our simulations, only the overall effect on the first excited state peak is analyzed. Absorption spectra were modeled in a similar way by Potter *et al.*[62] They reproduced the absorption due to the lowest excited state for samples using the average particle diameter determined by TEM. In our analysis, we deduce the particle size distribution by simulating the optical data and using an average effective mass from the literature. We emphasize that the purpose of this exercise is to elucidate the properties of the size distribution and its evolution for several series of samples heat treated at different temperatures and time. A more complete optical model would include more details such as size-dependent oscillator strength and more complex valence-band structure but our purpose here is to determine the trends with treatment rather than to test the theory.

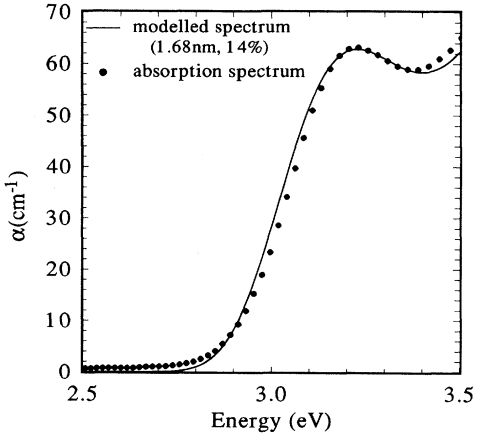

FIG. 7. Simulated spectrum and data for sample heat treated at $T=600$ °C and time 4 h.

The absorption for the composite is found by summing the absorption for each particle size; $\alpha(h\nu,R)$ multiplied by a weighting function for the particle size distribution, $N(R)$:

$$\alpha(h\nu)=\sum_R N(R)\alpha(h\nu,R) . \quad (8)$$

We find that we can get satisfactory agreement with experiment with the assumption of a Gaussian particle size distribution with standard deviation ΔR and center R.

We take each heat treatment temperature separately and determine the best fit parameters for mean particle size and width of the distribution in percent of particle size ($\Gamma=\Delta R/R*100$). Γ is directly related to the width of the first absorption peak, R is related to the position. A typical simulation of an absorption curve is shown in Fig. 7 together with the curve modeled. As a result, an

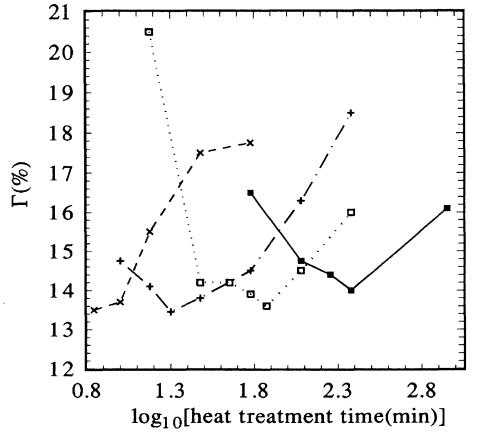

FIG. 8. Particle size distribution width (Γ), determined by simulation of data, plotted against heat treatment time. ■, 600 °C; □, 625 °C; +, 650 °C; ×, 675 °C.

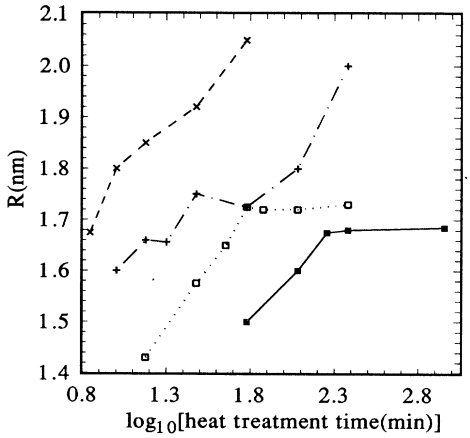

FIG. 9. Average particle radius, determined by simulation of the optical data, plotted against heat treatment time. ■, 600 °C; □, 625 °C; +, 650 °C; ×, 675 °C.

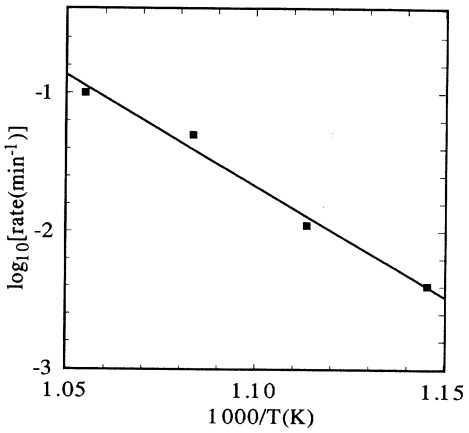

FIG. 10. Rate of increase of optical absorption in the nucleation regime plotted against $1000/T$.

average particle radius R and a particle size distribution ΔR were obtained for all optical-absorption spectra.

In Fig. 8 we plot the width of the size distribution (Γ) against the logarithm of heat treatment time. In Fig. 9 we plot average particle size R determined by simulation against the logarithm of heat treatment time. We see that the fractional width of the distribution decreases to a minimum at 7, 20, 70, and 200 min for $T=675$, 650, 625, and 600 °C, respectively. We note that the particle size distribution is narrowest just before the absorption peak reaches its maximum value for each temperature (see Fig. 4).

EVOLUTION OF THE SIZE DISTRIBUTION WITH TIME

As we discussed in the Introduction, in the standard model for particle growth we expect several possible stages of evolution of the particle distribution: Either nuclei are extrinsic or formed by homogeneous nucleation. Growth will follow the nucleation stage. If Cd or S are depleted before nucleation is complete, then the growth of the average radius will be at the expense of smaller particles and the distribution will widen.

The substantial increase in the magnitude of the absorption in the energy range from 3.1 to 3.5 eV at the early stages of the heat treatment must be due to an increase in the number of particles with radius between 1.6 and 1.8 nm. The way in which this peak appears and grows in a narrow size range is consistent with homogeneous nucleation. When the rate at which nucleation occurs exceeds the growth and dissolution rates, then the average particle radius will be nearly equal to the critical radius[44] and it will not change with time. In Figs. 1, 3, and 4 we see that there is a period for all samples with $T<675$ °C during which the peak grows but does not shift. In Fig. 10 we plot the rate at which the peak grows against the inverse temperature. A straight line through the points gives an activation energy of 3.5 ± 0.4 eV. In the homogeneous model, this energy corresponds to the sum of the free energy to form a critical nucleus plus the free energy for an atom to cross the interface.

If the absorption peak at 3.1–3.5 eV represents the critical nucleus size, then Eq. (2b) predicts that the inverse of average particle size in this peak plotted against heat treatment temperature will form a straight line with $1/R=0$ intercept at the equilibrium temperature T_0. In Fig. 11 we show the inverse of the average particle size in this time-independent regime plotted against heat treatment temperature. We expect a straight line through the R data which has an intercept at 1000 °C because we know that the equilibrium temperature must be between 900 and 1100 °C (particles can be dissolved in this range). Although a straight line can be placed through the data, the actual intercept is at higher temperature ($\sim$1500 °C).

Equation (4) predicts that the width of the particle size distribution during the nucleation stage depends only on temperature and surface tension. We observe a minimum width of $\Gamma=13-14\%$ or $\Delta R=0.22$ nm for the sample heat treated at 600 °C with $R=1.6$ nm. This yields a sur-

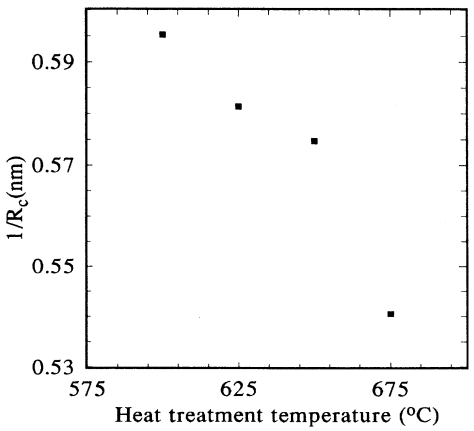

FIG. 11. Inverse of the average particle radius in the nucleation regime, plotted against heat treatment temperature.

face tension of 0.032 J/m^2 or approximately 0.2 eV/surface atom. Liu and Risbud[45] reported $\sigma=8.7\times10^{-4}$ J/m^2, approximately 40 times smaller than the present experiment. We do not yet know the origin of this discrepancy, but perhaps Se content in their samples is important. The width of our measured distribution increases slightly with increasing temperature from 0.22 nm for $T=600$ °C to 0.24 nm for $T=675$ °C, consistent with Eq. (4). The absolute energy width of the optical-absorption peak is narrower for higher temperatures because the absolute particle size is larger. Taking $\sigma=0.032$ J/m^2 and $R_c=1.6$ nm and using Eq. (2a), we find $\Delta G_v=4\times10^7$ J/m^3. We find the energy necessary to form a critical nucleus of 3.3 eV from the product of ΔG_v and critical volume. This energy is in good agreement with the activation energy of the rate of nucleus formation of 3.5 eV from above.

As nucleation proceeds, the concentration of reactants in the glass matrix decreases. As a result, the nucleation rate decreases and the critical nucleus size increases, leading to dissolution of smaller particles and an increase in the average particle size. The total number of particles will begin to decrease at this stage and the magnitude of the peak in the absorption coefficient will also decrease. During the time at which the nucleation rate exceeds the growth and dissolution rates before the concentration drops below a critical level Eqs. (2)–(4) apply. Once the number of particles begins to decease, as evidenced by a decrease in the absorption peak magnitude, the coarsening stage, described by Eq. (5), has set in.

It is clear from the spectra that unstruck glass contains quenched-in particles which have a very wide lowest excited state distribution. The total number of such particles with lowest excited state below 4 eV must be relatively small because the absorption coefficient is low. If this distribution constitutes the nuclei (rather than the nuclei being formed homogeneously), then we would expect normal diffusion-controlled growth to proceed immediately. In diffusion controlled growth, Eqs. (1) and (7) can be combined to yield

$$E_{\text{peak}}=E_{\text{bulk}}+A/t\ , \tag{9}$$

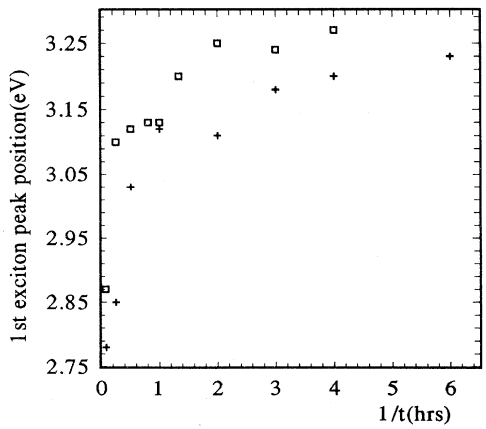

FIG. 12. E_{peak} vs $1/t$ for CdS/glass samples heat treated at 625 °C (□) and 650 °C (+).

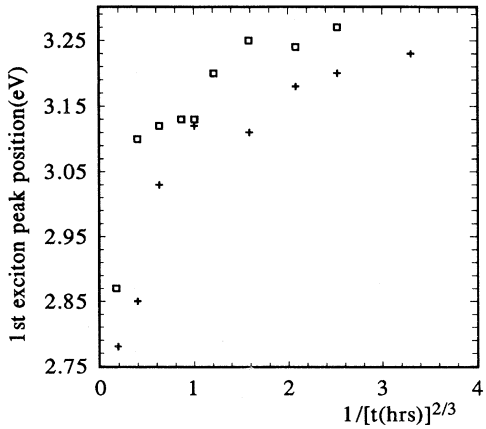

FIG. 13. E_{peak} vs $1/t^{2/3}$ for CdS/glass samples heat treated at 625 °C (□) and 650 °C (+).

where A is a constant. We expect E_{peak} to vary linearly in $1/t$ and for the intercept at $1/t=0$ to be E_{bulk}. In Fig. 12 we plot E_{peak} against $1/t$. Although it is possible to draw a straight line through portions of the data, none of the possible intercepts are close to the bulk band gap. For example, for the 625 °C series, the intercept for data with $t<8$ h is <3.1 eV, well above the band gap of our highest Zn sample. For the 650 °C series, the intercept is also close to 3.1 eV. The effect of Zn concentration on the band gap therefore cannot by itself account for the large intercept. In short, the rate at which the band gap shifts toward the bulk gap is inconsistent with simple diffusion-limited growth.

In the coarsening stage, Eq. (5) predicts that the average particle size increases as $t^{1/3}$ and the band gap will therefore vary according to

$$E_{\text{peak}}=E_{\text{bulk}}+Bt^{-2/3}\ . \tag{10}$$

In Fig. 13 we plot the position of the shoulder or peak in the data against $t^{-2/3}$. For long times and higher temperatures, it is possible to identify a straight line region which intercepts the $1/t=0$ axis near the bulk band gap.

SUMMARY

We have observed the evolution of the optical-absorption properties of CdS-doped glasses. After quenching from a high-temperature melt, the glasses are transparent in the visible and have only weak absorption for photon energy below 4 eV. With heat treatment, the optical-absorption coefficient increases and the absorption edge shifts to lower energy. We modeled the absorption spectra using a simple confined-particle model in order to convert optical-absorption data into particle-size distribution information.

For early stages of heat treatment, we observe that (i) the average particle size at each temperature is constant for an extended period while (ii) the number of particles of the average size increases, and (iii) the average particle size is a weak function of heat treatment temperature, increasing with increasing temperature. These observa-

tions are consistent with homogeneous nucleation by thermodynamic fluctuation of the dopant concentration and they are inconsistent with preexisting nuclei. Analyzing the data using homogeneous nucleation theory, the average particle radius of 1.6 nm at 600 °C indicates a Gibbs free energy of crystallite formation of 5×10^{-19} J (3.3 eV). The full width at half maximum of 0.22 nm at 600 °C is consistent with surface tension of 0.032 J/m^2. The critical temperature is 900–1100 °C. The narrowest relative size distributions, and the narrowest optical-absorption peaks, are found during the homogeneous nucleation stage. The activation energy for the rate of particle formation is 3.5 eV. The critical radius increases linearly with heat treatment temperature; smaller particles can be prepared by treatment at lower temperature, but the treatment time goes up exponentially and it is not practical to grow particles below 550 °C.

As time progresses, the absorption peak reaches a maximum value of 50 cm^{-1} for all temperatures (600–675 °C) and then begins to decrease as the absorption peak shifts to lower energy. At the same time, the particle-size distribution begins to broaden. After long times the absorption peak becomes a shoulder and the spectrum approaches that of bulk $Cd_{1-x}Zn_xS$. We interpret this stage, when the absorption peak decreases in magnitude, as the ripening or coarsening stage. The observed absorption edge shift and particle distribution broadening at later times are consistent with the predictions of the Lifshitz-Slyozov theory.

We also observe that the Raman peak shifts upward from 303 cm^{-1} at short times to 315 cm^{-1} as heat treatment progresses. We propose that the Zn content of the nanoparticles increases with time to a maximum level of about 0.15. Measurements with different laser lines resonant with different portions of the spectrum of a single sample indicate that the Zn content does not depend on particle size. This suggests that Zn content of any given particle does not depend on the history or age of the particle. We propose, therefore, that the Zn content depends only on the ratio of Zn to Cd in the glass. The maximum Zn incorporation increases the band gap of the bulk alloys slightly from 2.45 to 2.65 eV.

CONCLUSIONS

We have shown how confinement-induced shifts in the optical transition energies of semiconductor nanoparticles can be used to study the nucleation and growth behavior of CdS alloy particles in glass. We observe well-defined sharp optical-absorption peaks only during the earliest stage of particle growth, which we identify as the homogeneous nucleation stage on the basis of the evolution of the spectrum with time. The width of the optical peak is directly related to the size distribution. In homogeneous nucleation theory the width of the size distribution is determined by the ratio of heat treatment temperature to interface tension.

Theory thus predicts that slightly narrower distributions can be generated by lower temperature heat treatment. It is possible that greater gains can be made by modifying the glass composition in order to raise the interface tension. Finally, separating the nucleation and growth stages from one another by addition of impurities or multitemperature treatment continues to be a promising approach.

ACKNOWLEDGMENTS

We gratefully acknowledge support of this research by NSF Grant Nos. DMR-9006956, 9104086, and 8801004. X-ray-absorption measurements were made at SSRL, which is funded by the DOE Office of Basic Energy Sciences and the NIH Biotechnology Resource Program. We thank Schott Glass Technologies for providing the unstruck doped glass. The first author (H.Y.) was supported by the Ministry of Education of the Republic of Türkiye. We thank L. Lurio, J. Pant, J. Riordan, J. Schroeder, M. Silvestri, M. Stapleton, and K. Stokes for assistance with experimental measurements and helpful discussions.

[1]N. F. Borrelli, D. Hall, H. Holland, and D. Smith, J. Appl. Phys. **61**, 5399 (1987).
[2]B. Fluegel, *et al.*, J. Cryst. Growth **101**, 643 (1990).
[3]C. Flytzanis, F. Harbe, M. C. Klein, and D. Ricard, SPIE Proc. Opt. Complex Syst. **1319**, 75 (1990).
[4]A. Gabel, K. W. DeLong, C. T. Seaton, and G. L. Stegemann, Appl. Phys. Lett. **51**, 1682 (1987).
[5]F. Henneberger, J. Puls, C. Spiegelberg, A. Schulzgen, H. Rossman, V. Jungnickel, and A. I. Ekimov, Semicond. Sci. Technol. **16**, A41 (1991).
[6]R. Jain and R. C. Lind, J. Opt. Soc. Am. **73**, 647 (1983).
[7]H. Jerominek, S. Patela, M. Pidgeon, Z. Jakubzyk, C. Delisle, and R. Tremblay, J. Opt. Soc. Am. B **5**, 496 (1988).
[8]J. T. Remillard, H. Wang, M. D. Webb, and D. G. Steel, J. Opt. Soc. Am. B **7**, 897 (1990).
[9]Y. Wang and N. Heron, J. Phys. Chem. **95**, 525-532 (1991).
[10]L. E. Brus, in *Proceedings of NATO Advanced Study Institute School on Nanophase Materials,* edited by G. C. Hadjipanayis (Kluwer Academic, London, 1993).
[11]H. Shinojima, J. Yumoto, and N. Uesugi, Appl. Phys. Lett. **60**, 298 (1992).
[12]L. Brus, Appl. Phys. A **53**, 465 (1991).
[13]J. Warnock and D. D. Awschalom, Appl. Phys. Lett. **48**, 425 (1986).
[14]S. Schmitt-Rink, D. A. B. Miller, and D. Chemla, Phys. Rev. B **35**, 8113 (1987).
[15]M. C. Schanne-Klein, F. Hache, D. Ricard, and C. Flytzanis, J. Opt. Soc. Am. B **51**, 2234 (1992).
[16]P. Roussignol, D. Ricard, and C. Flytzanis, Appl. Phys. B **51**, 437 (1990).
[17]S. V. Gaponenko, U. Woggon, M. Saleh, W. Langbein, A. Uhrig, M. Muller, and C. Klingshirn, J. Opt. Soc. Am. B **10**, 1947 (1993).
[18]S. S. Yao, C. Karaguleff, A. Gabel, R. Fortenberry, C. T.

Seaton, and G. I. Stegemann, Appl. Phys. Lett. **46**, 801 (1985).
[19]D. Ricard, M. Ghanassi, and M. C. Schanne-Klein, Opt. Commun. **108**, 311 (1994).
[20]D. M. Mittlemen, R. W. Schoenlein, J. J. Shiang, V. L. Colvin, A. P. Alivisatos, and C. V. Shank, Phys. Rev. B **49**, 14 435 (1994).
[21]M. G. Bawendi, P. Carroll, W. L. Wilson, and L. E. Brus, J. Chem. Phys. **96**, 946 (1992).
[22]C. B. Murray, D. J. Norris, and M. G. Bawendi, J. Am. Chem. Soc. **115**, 8706 (1993).
[23]P. D. Persans, A. Tu, Y. J. Wu, and M. Lewis, J. Opt. Soc. Am. B **6**, 818 (1989).
[24]B. G. Potter and J. H. Simmons, Phys. Rev. B **37**, 10 838 (1988).
[25]B. G. Potter and J. H. Simmons, J. Appl. Phys. **68**, 1218 (1990).
[26]M. Ferrari, B. Champagnon, and M. Barland, J. Non-Cryst. Solids **151**, 95 (1992).
[27]M. Steigerwald and L. Brus, Ann. Rev. Mater. Sci. **19**, 471 (1989).
[28]A. I. Ekimov, A. L. Efros, and A. A. Onuschchenko, Solid State Commun. **56**, 921 (1985).
[29]D. Norris, M. Nirmal, C. Murray, A. Sacra, and M. Bawendi, Z. Phys. D **26**, 355 (1993).
[30]A. I. Ekimov, A. A. Onushchenko, and V. A. Tsekhomskii, Fiz. Khim. Stekla **6**, 511 (1980).
[31]A. I. Ekimov and A. A. Onuschchenko, Pis'ma Zh. Eksp. Teor. Fiz. **34**, 363 (1981) [JETP Lett. **34**, 345 (1981)].
[32]P. D. Persans, M. Silvestri, G. Mei, E. Lu, H. Yukselici, and J. Schroeder, Braz. J. Phys **23**, 144 (1993).
[33]W. A. Weyl, *Coloured Glasses* (Dawsons of Pall Mall, London, 1959).
[34]J. A. Williams, G. E. Rindone, and H. A. McKinstry, J. Am. Chem. Soc. **64**, 702 (1981).
[35]Y. Fuyu and J. M. Parker, Mater. Lett. **6**, 233 (1988).
[36]P. Persans, A. Tu, M. Lewis, T. Driscoll, and R. Redwing, in *Materials Issues in Microcrystalline Semiconductors,* Materials Research Society Symposia No. 164, edited by P. Fauchet, C. C. Tsai, and K. Tanaka (MRS, Pittsburgh, 1990), p. 105.
[37]J. A. M. Neto, L. G. Barbosa, C. L. Cesar, O. L. Avles, and F. Galembeck, Appl. Phys. Lett. **59**, 2715 (1991).
[38]R. H. Doremus, *Glass Science* (Wiley, New York, 1994).
[39]L. Landau and E. Lifshitz, *Statistical Physics* (Pergamon, Oxford, 1980), Vol. 5.
[40]S. A. Gurevich, A. I. Ekimov, I. A. Kudryavtsev, O. G. Lyublinskaya, A. V. Osinskii, A. S. Usikov, and N. N. Faleev, Semiconductors **28**, 486 (1994).
[41]D. Turnbull, in *Solid State Physics,* edited by F. Seitz and D. Turnbull (Academic, New York, 1956).
[42]D. Turnbull, J. Appl. Phys. **21**, 1022 (1950).
[43]E. M. Lifshitz and L. P. Pitaevskii, *Physical Kinetics* (Pergamon, Oxford, 1981), Vol. 10.
[44]R. Kampmann and R. Wagner, *Decomposition of Alloys: The Early Stages* (Pergamon, Oxford, 1984), p. 91.
[45]L.-C. Liu and S. H. Risbud, J. Appl. Phys. **68**, 28 (1990).
[46]I. M. Lifshitz and V. V. Slyozov, J. Phys. Chem. Solids **19**, 35 (1961).
[47]V. Sukumar and R. H. Doremus, Phys. Status Solidi B **179**, 307 (1993).
[48]M. Silvestri, Ph.D. thesis, Rensselaer Polytechnic Institute (1994).
[49]T. Hayes, L. Lurio, R. J. Olsson, J. Pant, H. Yükselici, and P. Persans, Physica B **208/209**, 585 (1994).
[50]P. D. Persans, L. B. Lurio, J. Pant, R. J. Olsson, H. Yukselici, and T. M. Hayes, in *Microcrystalline and Nanocrystalline Semiconductors,* Materials Research Society Symposia No. 358, edited by R. Collins, C. C. Tsai, M. Hirose, F. Koch, and L. Brus (MRS, Pittsburgh, 1995), p. 225.
[51]A. Tu and P. Persans, Appl. Phys. Lett. **58**, 1506 (1991).
[52]A. Tu, Ph.D. thesis, Rensselaer Polytechnic Institute (1991).
[53]E. Lu, Ph.D. thesis, Rensselaer Polytechnic Institute (1993).
[54]*Properties of II-VI Compounds,* edited by K.-H. Hellwege and O. Madelung, Landolt-Börnstein, New Series, Group III, Vol. 17, Pt. h (Springer-Verlag, Berlin, 1985).
[55]X. S. Zhao, J. Schroeder, P. Persans, and E. Lu, in *Materials Issues in Microcrystalline Semiconductors* (Ref. 36), p. 93.
[56]X. S. Zhao, J. Schroeder, P. Persans, and T. Bilodeau, Phys. Rev. B **43**, 12 580 (1991).
[57]J. Schroeder, M. Silvestri, X. S. Zhao, P. Persans, and L. W. Hwang, in *Chemical Processes in Inorganic Materials: Metal and Semiconductor Clusters and Colloids,* Material Research Society Symposia No. 272, edited by P. Persans, J. Bradley, R. Chianelli, and G. Schmidt (MRS, Pittsburgh, 1992), p. 251.
[58]H. Richter, Z. P. Wang, and L. Ley, Solid State Commun. **39**, 625 (1981).
[59]P. M. Fauchet and I. H. Campbell, Crit. Rev. Solid State Mater. Sci. **14**, S79 (1988).
[60]L. K. Vodop'yanov, B. S. Umarov, L. A. Sysoev, and L. A. Sarkisov, Pis'ma Zh. Eksp. Teor. Fiz. **13**, 507 (1971) [JETP Lett. **13**, 660 (1971)].
[61]G. B. Grigoryan, E. M. Kazaryan, A. I. Efros, and T. V. Yazeva, Fiz. Tverd. Tela (Leningrad) **32**, 1772 (1990) [Sov. Phys. Solid State **32**, 1031 (1990)].
[62]B. G. Potter, J. H. Simmons, P. Kumar, and C. J. Stanton, J. Appl. Phys. **75**, 8089 (1994).